Properties of a 4Pi confocal fluorescence microscope

Stefan Hell and Ernst H. K. Stelzer

Light Microscopy Group, European Molecular Biology Laboratory, Meyerhofstrasse 1, D-6900 Heidelberg, Germany

Received April 15, 1992; accepted June 10, 1992; revised manuscript received June 29, 1992

In a 4Pi confocal fluorescence microscope two opposing microscope objective lenses were used to illuminate a fluorescent object from both sides and to collect the fluorescence emissions on both sides. Constructive interference of either the illumination wave fronts in the common focus or the detection wave fronts in the common detector pinhole resulted in an axial resolution approximately four times higher than that in a confocal fluorescence microscope. A precise 4Pi confocal fluorescence microscope that uses simultaneous illumination was built. The full width at half-maximum of the depth discrimination was determined experimentally to be approximately 110 nm when lenses with a numerical aperture of 1.4, an excitation of 633 nm, and detection of approximately 725 nm were used.

INTRODUCTION

The resolution of a confocal fluorescence microscope is determined by the extent of the confocal three-dimensional point-spread function.[1] For pointlike illumination and detection, the volume of the point-spread function depends on the numerical aperture of the microscope objective and on the wavelengths of the emission and the excitation light.[1,2] The smaller this volume, the better the resolution of the microscope. In the usual confocal and conventional epifluorescence arrangement, the object is illuminated and observed from one side (Fig. 1). The objective lens transforms the illumination wave front into a segment of a spherical wave front. For technical reasons, the maximum aperture of an oil immersion lens is 1.4, i.e., the aperture angle is below $2 \times 68° = 136°$.[3,4] This fact leads to a geometry for the point-spread-function volume that is extended along the optical axis. If the illumination is uniformly spherical, the resultant spot becomes round and has a diameter somewhat larger than $\lambda/2$. If this ideal illumination is approached and if two microscope objectives of high numerical aperture are used, a fluorescent sample can be illuminated coherently from both sides, and the fluorescence emission is also detected on both sides. This arrangement is equivalent to an increase of the aperture along the axial direction. The result is a point-spread function with a geometry that is determined by the pattern of two wave fronts interfering in a common focal volume. In the case of constructive interference, the axial extent of the confocal point-spread function is reduced; this reduction is equivalent to an improved axial resolution.[5-7] A technique that relies on this principle has been described in Ref. 5. A related approach to reflection microscopy, in which a double-pass confocal microscope is used, has been independently described and demonstrated elsewhere.[8]

THEORY

In a confocal fluorescence microscope, a point light source and a point detector are used to observe a fluorescently labeled specimen.[9-11] As a result of diffraction, the illuminating wave front forms a three-dimensional intensity distribution in the vicinity of the focal spot. This phenomenon is described physically by the point-spread function of the microscope objective lens.[12]

For high numerical apertures, a theory that takes the electromagnetic properties of light into account must be used.[13,14] According to Richards and Wolf,[15-17] the normalized electric field of linearly polarized light in the focal region of an aplanatic system can be quantified as

$$\mathbf{E} = (e_x, e_y, e_z), \tag{1a}$$

with

$$\begin{aligned} e_x(\mathbf{r}) &= -i(I_0 + I_2 \cos 2\phi), \\ e_y(\mathbf{r}) &= -iI_2 \sin 2\phi, \\ e_z(\mathbf{r}) &= -2I_1 \cos \phi. \end{aligned} \tag{1b}$$

ϕ defines the azimuth angle between the initial direction of vibration of the incident field and the direction of observation; $\mathbf{r}$ is the coordinate originating in the geometrical focus; and I_0, I_1, and I_2 are integrals (defined in Ref. 16) over the objective lens aperture, depending on the aperture angle and the wavelength, with I_1 and I_2 vanishing for low numerical apertures.

Equations (1) suggest that, for high numerical apertures and illumination with linearly polarized light, the electric field is not cylindrically symmetric around the optical axis. For $\phi = \pi/2$ (corresponding to the direction perpendicular to the direction of vibration of the incident electric field), the point-spread function is narrower than for $\phi = 0$.[16] Hence the time-averaged illumination-intensity distribution in the focal region for linearly polarized illumination is given by[18]

$$\begin{aligned} I = h_{\mathrm{ill}} &= |\mathbf{E}|^2 \\ &= |I_0|^2 + 4|I_1|^2 \cos^2 \phi + |I_2|^2 + 2 \cos 2\phi \, \mathrm{Re}(I_0 I_2^*). \end{aligned} \tag{2}$$

Equation (2) is also referred to as the illumination point-spread function of the confocal microscope. Figure 2 shows the normalized illumination-intensity distribution along the optical axis for $\phi = \pi/2$, N.A. = 1.4 (oil), and an excitation wavelength of 633 nm.

In the calculation of the detection point-spread function it is assumed that the fluorescent light is randomly

0740-3232/92/122159-08$05.00

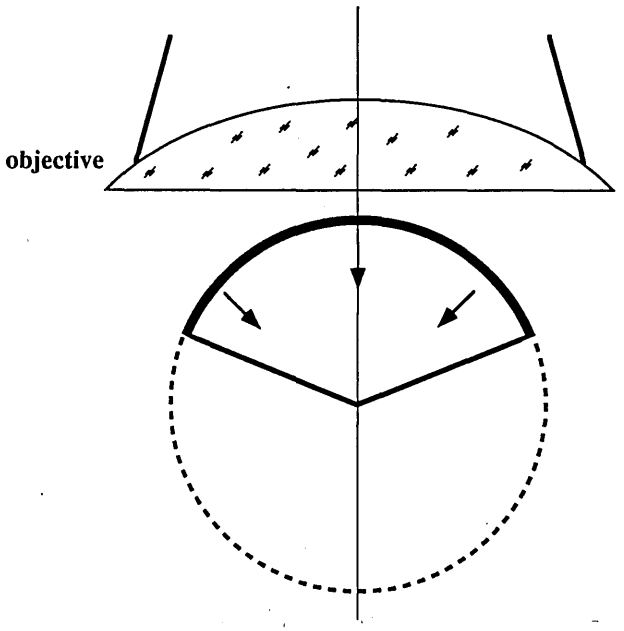

Fig. 1. Aperture angle in microscopy. In the usual epifluorescence arrangement, always less than half of 4π is used to illuminate the point of interest and to detect the emitted light.

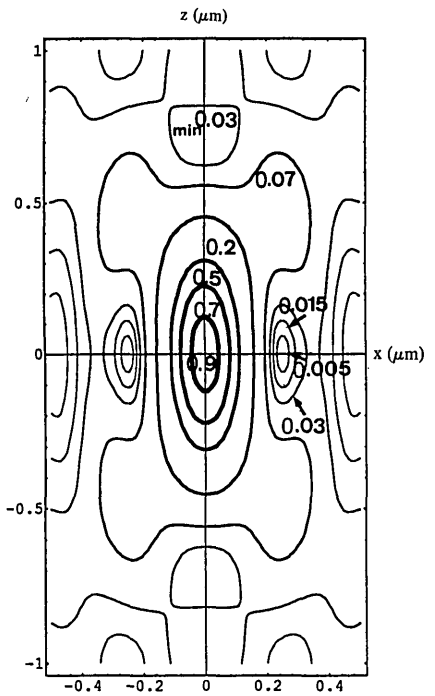

Fig. 2. Contour plot of the point-spread function for linearly polarized illumination. The horizontal axis lies in the focal plane and is perpendicular to the direction of vibration of the incident electric field. The numerical aperture of the oil ($n = 1.518$) immersion lens is 1.4; the wavelength is 633 nm. The point-spread function is normalized to unity. The contour lines drop as follows: 0.9, 0.7, 0.5, 0.2, 0.07, 0.03, 0.015, and 0.005. They are indicated by decreasing line thicknesses. This applies to all contour plots shown in this paper.

polarized and has a wavelength of 725 nm. This condition yields the somewhat different point-spread function[19] shown in Fig. 3:

$$h_{\mathrm{det}} = |I_0|^2 + 2|I_1|^2 + |I_2|^2. \tag{3}$$

The confocal point-spread function is given by the product of the two point-spread functions and is denoted by H:

$$H = h_{\mathrm{ill}} h_{\mathrm{det}}. \tag{4}$$

The function H is proportional to the probability of an illumination photon's both exciting a fluorophore in the vicinity of the geometrical focus and detecting a photon emitted from the same position.[6,20]

The basic idea of the 4Pi confocal fluorescence microscope is to use two microscope objectives with a common focus to increase the aperture of the microscope. An increase of the aperture along the axial direction is achieved either when the objectives are illuminated with coherent wave fronts that are interfering constructively in the common focus or when the fluorescent light that is collected from both sides interferes constructively in the common point detector. Since a solid angle of 4π is not achievable, the term 4Pi was chosen to indicate the basic idea with a simple and straightforward term.

Apart from operating as a confocal fluorescence microscope, the 4Pi confocal fluorescence microscope comprises three different types of imaging that feature a higher resolution:

Type A: The two illuminating wave fronts interfere in the sample (4Pi illumination):

$$H_{\mathrm{4Pi,ill}} = |\mathbf{E}_{1,\mathrm{ill}} + \mathbf{E}_{2,\mathrm{ill}}|^2 |\mathbf{E}_{\mathrm{det}}|^2. \tag{5}$$

Type B: The two detection wave fronts interfere in the detector (4Pi detection):

$$H_{\mathrm{4Pi,det}} = |\mathbf{E}_{\mathrm{ill}}|^2 |\mathbf{E}_{1,\mathrm{det}} + \mathbf{E}_{2,\mathrm{det}}|^2. \tag{6}$$

Type C: Both the illuminating and the detecting wave fronts interfere (4Pi illumination and 4Pi detection):

$$H_{\mathrm{4Pi,4Pi}} = |\mathbf{E}_{1,\mathrm{ill}} + \mathbf{E}_{2,\mathrm{ill}}|^2 |\mathbf{E}_{1,\mathrm{det}} + \mathbf{E}_{2,\mathrm{det}}|^2. \tag{7}$$

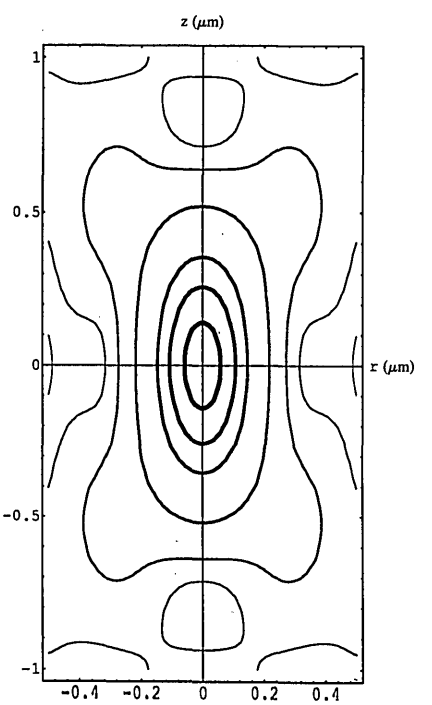

Fig. 3. Contour plot of the detection point-spread function. The numerical aperture of the lens is 1.4, the detection wavelength is 725 nm, and the index of refraction is $n = 1.518$.

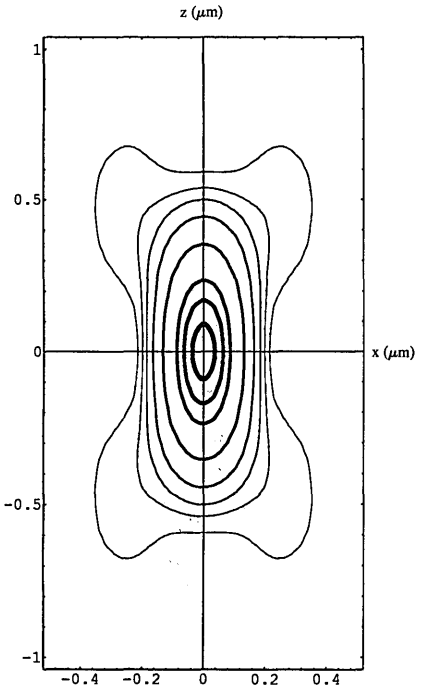

Fig. 4. Contour plot of the confocal point-spread function. It is the product of the functions shown in Figs. 2 and 3.

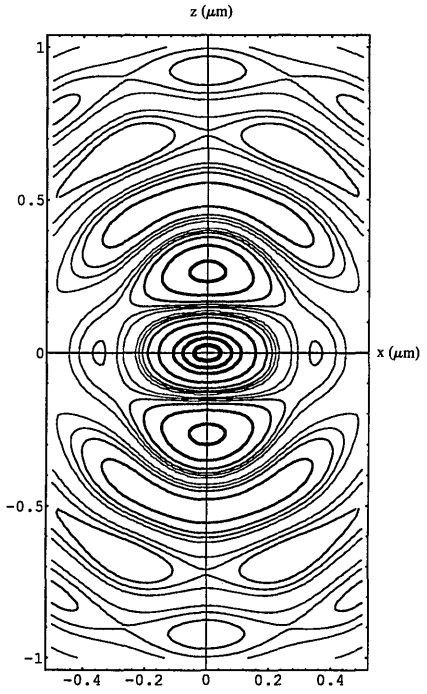

Fig. 5. Contour plot of the illumination point-spread function in a type-A 4Pi confocal fluorescence microscope. The two illumination wave fronts interfere constructively in the common focus. Both lenses have a numerical aperture of 1.4; the wavelength is 633 nm. The wave fronts are linearly polarized, and the x axis is perpendicular to the plane of vibration of the incident electric field.

THEORETICAL RESULTS

Contour plots of the different point-spread functions are shown in Figs. 2–8. Figure 5 illustrates the illumination point-spread function for a 4Pi confocal fluorescence microscope that uses two microscope objectives of N.A. = 1.4 (oil) and $\lambda = 633$ nm and linearly polarized light. The horizontal observation axis is perpendicular to the plane of vibration of the excitation light ($\phi = \pi/2$). The first minimum along the axial direction is found at $z = \pm 142$ nm away from the focal point. This is five times

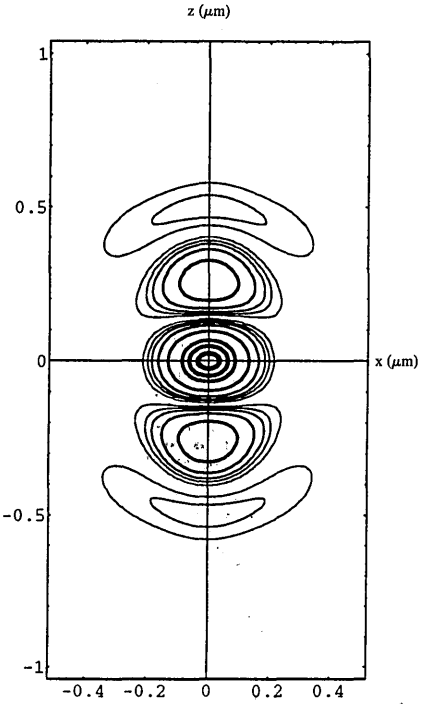

Fig. 6. Contour plot of the confocal point-spread function in a type-A 4Pi confocal fluorescence microscope. This point-spread function is calculated by multiplying the point-spread function for the normal detection (Fig. 3) and the point-spread function shown in Fig. 5.

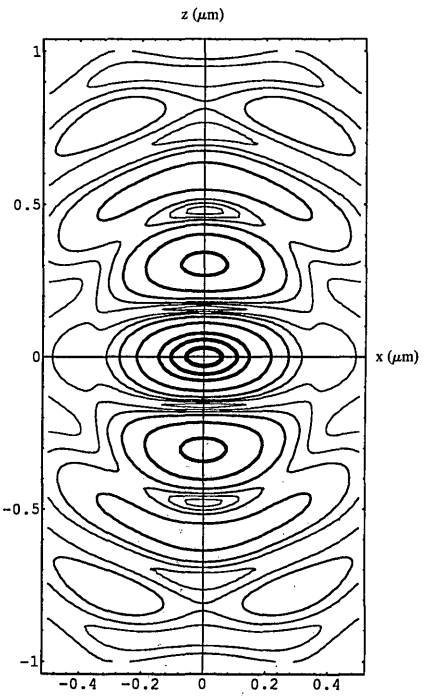

Fig. 7. Contour plot of the detection-intensity point-spread function in a type-B or type-C 4Pi confocal fluorescence microscope.

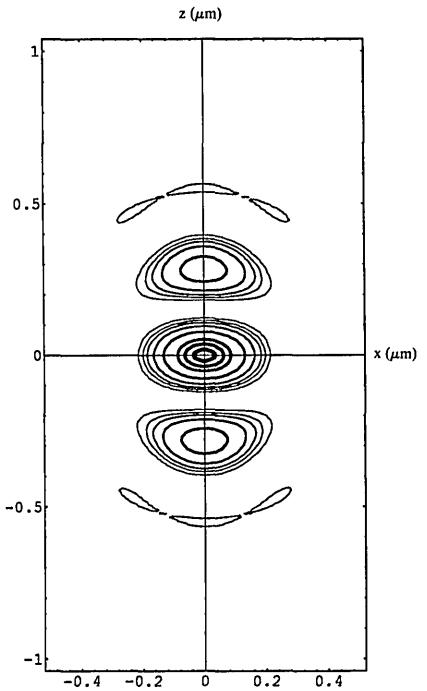

Fig. 8. Contour plot of the confocal point-spread function in a type-C 4Pi confocal fluorescence microscope. This point-spread function is calculated by multiplying the point-spread functions shown in Figs. 5 and 7.

less than in the case of normal illumination with the first minima at $z = \pm 705$ nm. However, the lack of a complete spherical wave front and the presence of aplanatic illumination force additional elevations along the optical axis that reach peak values of 0.58.

For calculation of the resolution of the type-A 4Pi confocal fluorescence microscope (4Pi illumination and normal detection), the illumination point-spread function as shown in Fig. 5 must be multiplied by the detection point-spread function as it is shown in Fig. 3. The result is displayed in Fig. 6, where the confocal point-spread function for a type-A 4Pi confocal fluorescence microscope can be seen. The full width at half-maximum reaches a value of approximately 138 nm in axial direction, which is a great improvement in axial resolution. As a result of the multiplication with the detection point-spread function, the peak height of the axial side elevations is reduced to 0.4. These elevations, however, reduce the benefit of the improved full width at half-maximum.

Figure 7 shows the detection point-spread function for the constructive interference of the detection wave fronts. The longer wavelength and the random polarization lead to a detection point-spread function that is different from the illumination point-spread function shown in Fig. 5. Figure 8 shows the point-spread function for a type-C 4Pi confocal fluorescence microscope (4Pi illumination and 4Pi detection), with constructive interference assumed for both illumination and detection. The location of the first minimum is nearly the same as for a type-A 4Pi confocal fluorescence microscope, but the upper and lower elevations have the somewhat lower value of 0.32 (Table 1).

Confocal fluorescence microscopy is of interest mainly because of its ability to resolve object planes that are stacked vertically along the optical axis.[21,22] To quantify the axial resolution for planes, we calculated the intensity signal $I_{\text{layer}}(z)$ (z responses) for an infinitely thin fluorescent layer by integrating the three-dimensional point-spread function in the x–y plane:

$$I_{\text{layer}}(z) = \int_{-\infty}^{\infty}\int_{-\infty}^{\infty} h_{\text{ill}}(x, y, z)h_{\text{det}}(x, y, z)\mathrm{d}x\mathrm{d}y \qquad (8)$$

The calculated z responses of a confocal fluorescence microscope and a 4Pi confocal fluorescence microscope to a fluorescence layer along the optical axis are shown in Fig. 9. The full width at half-maximum of the central peak in axial direction for a type-A 4Pi confocal fluorescence microscope (N.A. = 1.4; λ = 633 nm) is 138 nm, while that for a comparable confocal fluorescence microscope is 540 nm. The heights of the side elevations along the optical axis direction reach a value of 0.46. The z response for a type-A 4Pi confocal fluorescence microscope is within the envelope of the z response of the confocal fluorescence microscope. For a type-C 4Pi confocal fluorescence microscope, these elevations have a value of 0.32, and the full width at half-maximum of the central peak is 105 nm.

The response to an infinitely steep edge can be computed by integrating the z response along the optical axis:

$$I_{\text{edge}}(z) = \int_{-\infty}^{z} I_{\text{layer}}(z')\mathrm{d}z' \qquad (9)$$

$I_{\text{edge}}(z)$ functions are shown in Fig. 10. They are of great interest because they can be measured by focusing into a homogeneously fluorescent thick object.

4PI CONFOCAL FLUORESCENCE MICROSCOPE

In the 4Pi confocal fluorescence microscope at the European Molecular Biology Laboratory, the optical system is at rest and the specimen is moved through the common focus of two microscope objective lenses. All the optomechanical parts are mounted upon a flat optical bench plate (Fig. 11). The light of a helium–neon laser is focused into a 10-μm pinhole (PH) and collimated with a 250-mm lens. This beam passes a dichroic (DC) beam splitter, is separated into two coherent beams of equal intensity in a beam-splitter cube, and is directed to the microscope objective lenses by further mirrors. The two beams are focused in a common focal plane. Fluorescent light that is emitted in all directions is collected by both lenses. The emission beams partially follow the path of the excitation light but are deflected toward the detector. A 250-mm

Table 1. Summary of Theoretical Predictions[a]

	Microscope		
Variable	CFM	4 Pi (Type A)	4 Pi (Type C)
Axial FWHM central peak	1	0.26	0.20
Total volume	1	0.50	0.32
Height, upper/lower elevation	—	0.46	0.32

[a]All calculations are normalized to the same height of the central peak. The numerical aperture of the oil (n = 1.518) immersion lenses is 1.4, the excitation wavelength is 633 nm, and the emission wavelength is 725 nm. CFM, confocal fluorescence microscope; FWHM, full width at half-maximum.

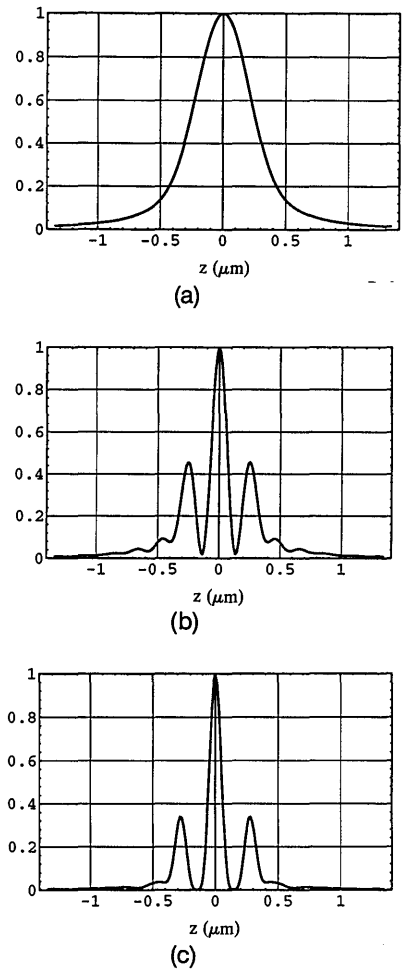

Fig. 9. Theoretical (z)responses to an infinitely thin fluorescent layer: (a) the response of a confocal fluorescence microscope, (b) the response of a type-A 4Pi confocal fluorescence microscope, (c) the response of a type-C 4Pi confocal fluorescence microscope. In all three cases, objective lenses with an N.A. of 1.4, an excitation wavelength of 633 nm, and an emission wavelength of 725 nm were assumed.

lens focuses the light into a 50-μm-diameter pinhole, a 3- or 6-mm thick RG665 long-pass filter rejects the 633-nm excitation light, and the fluorescence emission is detected with a red-sensitive Hamamatsu 647-01 photomultiplier.

Specimen movement is accomplished with a piezoelectrically driven scan stage (Photon Control, Cambridge, England) that offers independent x, y, and z axes. The maximal distance per axis is 20 μm, and the smallest resolvable step is 5 nm. While one of the microscope objective lenses is fixed, the position of the other lens is piezoelectrically adjustable along independent x, y, and z axes (Physik Instrumente, Waldbronn, Germany). The dichroic beam splitters are operated with an incidence angle of 45°, and, in contrast to most other dichroic beam splitters, transmit the 633-nm light of the laser, while 90% of the fluorescently emitted light above 650 nm is deflected.

EXPERIMENTAL RESULTS

To prove the principle of 4Pi confocal fluorescence microscopy and the predicted enhancement in axial resolution, we prepared a layer of Nile Blue A Perchlorate (Kodak Optical Products, CAS No.:53340-16-2) that was immersed in ethanol and mounted between two cover slides. This sample provides an edge along the optical axis. A saturated solution of Nile Blue was used to produce a good signal-to-noise-ratio (SNR). A transmission loss along a distance of 5 μm was below the detection limit.

The sample was placed between the two microscope objective lenses (Zeiss Planapochromat 63 × /1.4 oil or 100 × /1.4 oil) and was moved through their common focus. The size of the increments was 10 nm. The scan speed was 0.5 μm/s. The excitation power of the laser was reduced until no bleaching occurred. The measurements of the axial resolution were performed with fluorescent layers that were between 500 nm and 5 μm thick. The signal of interest was the response of the optical system to a step along the optical axis, i.e., the function $I_{\text{edge}}(z)$ as described by Eq. (9). We measured the response of the type-A 4Pi confocal fluorescence microscope with both objective lenses; we measured the confocal fluorescence response with a single objective lens by closing the other path.

Figure 12 shows the intensity signal for a 590-nm-thick fluorescent layer as a function of the position along the optical axis. The slopes correspond to the function $I_{\text{edge}}(z)$

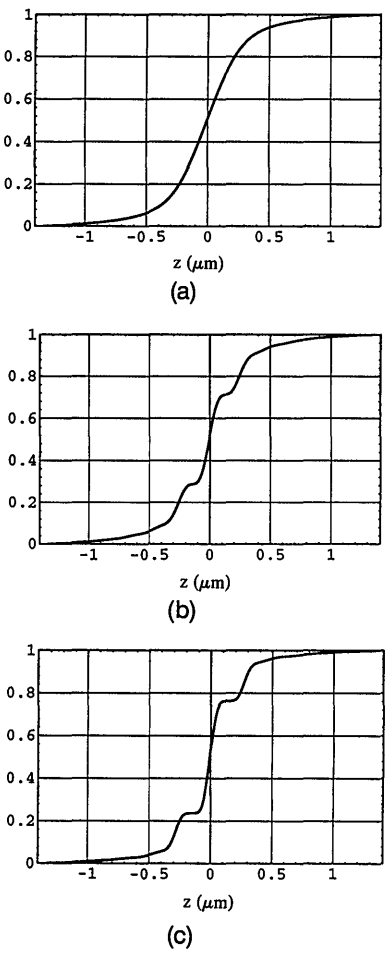

Fig. 10. Theoretical response to an edge along the optical axis: (a) the response of a confocal fluorescence microscope, (b) the response of a type-A 4Pi confocal fluorescence microscope, (c) the response of a type-C 4Pi confocal fluorescence microscope.

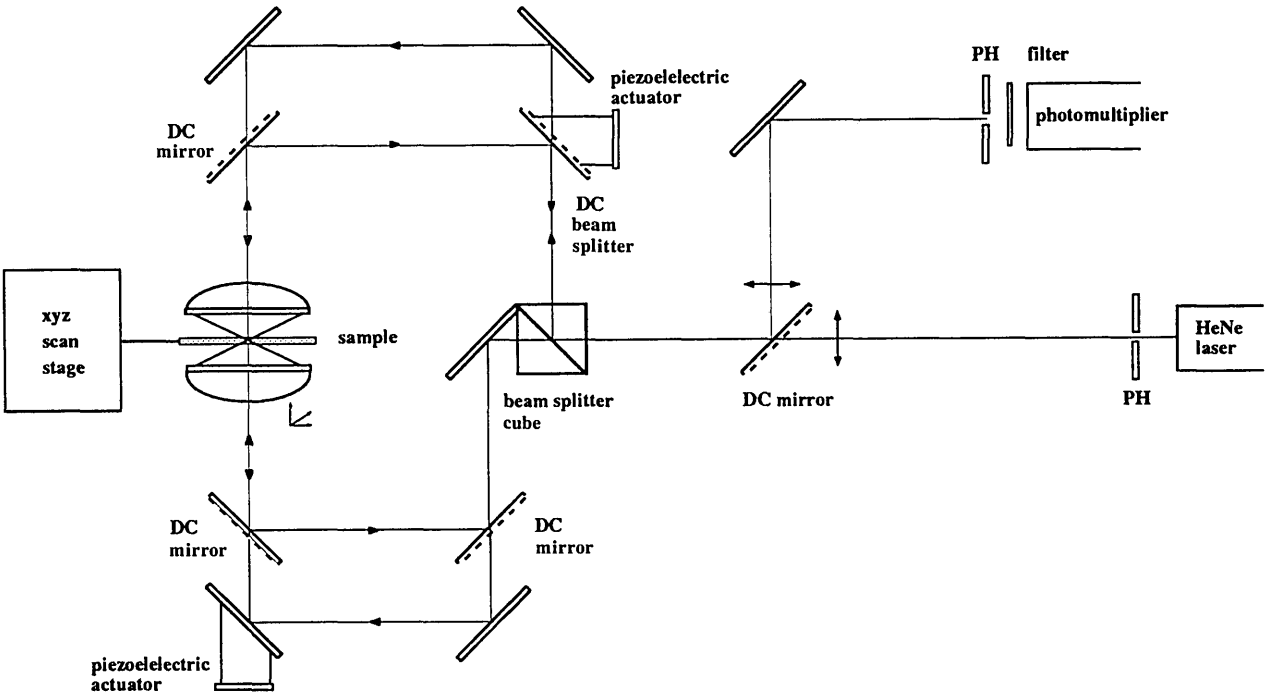

Fig. 11. Schematic drawing of the 4Pi confocal fluorescence microscope at the European Molecular Biology Laboratory.

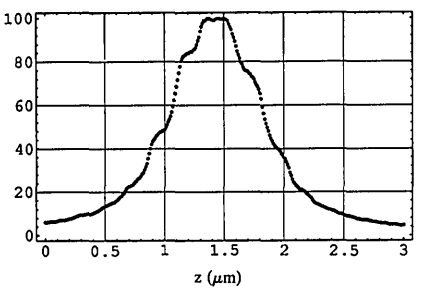

Fig. 12. Experimental response of a type-A 4Pi confocal fluorescence microscope to a 590-nm-thick fluorescent layer. The intensity is normalized to 100. The distance along the optical axis (z) is given in micrometers.

for the edges of the layer. Their first derivatives [i.e., the experimentally gained curve $I_{\text{layer}}(z)$ or z response] are shown in Fig. 13 for the type-A 4Pi confocal fluorescence microscope [Fig. 13(a)] and the confocal fluorescence microscope [Fig. 13(b)]. The experiment clearly demonstrates that the z responses for the type-A 4Pi confocal fluorescence microscope are within the envelope of the confocal fluorescence microscope z responses. Clearly distinguishable are the center peak and at least two upper and lower peaks [Fig. 13(b)]. The distance between the first two minima is 242 nm. The lower peak and the upper peak are, respectively, 235 and 195 nm apart from the main peak. The heights of the upper and lower peaks are between 62% and 66% of the central peak. The full width at half-maximum of the central peak is approximately 110 nm. The full width at half-maximum for the confocal fluorescence microscope is larger than 550 nm. All distances and lengths given are precise within a range of 20 nm, i.e., twice the movement increments that were used in these experiments. For this experiment the calculated full width at half-maximum for the confocal fluorescence microscope is 540 nm, the calculated distance between the first two minima is 270 nm, the theoretical heights of the axial side elevations are 46% of that of the central peak, and the theoretical full width at half-maximum of the central peak is 138 nm.

The phase was adjusted with the piezoelectrically driven mirror in the illumination path. Deliberate changes in phase caused the intensity steps to move along the slope. Two wave fronts that were not in phase resulted in asymmetrically sized upper and lower elevations as well as in

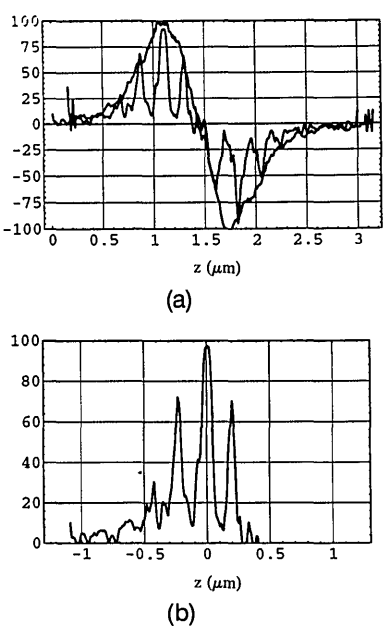

Fig. 13. First derivative of the experimental responses to a fluorescent layer shown in Fig. 12. (a) The z responses of the type-A 4Pi confocal fluorescence microscope and the z responses of the confocal fluorescence microscope (envelope), (b) the z response shown in the same scale as the theoretical predictions for this experiment.

smaller central peaks. In the case of destructive interference, the central peak vanished.

DISCUSSION AND OUTLOOK

A comparison of theory and data shows good agreement, which proves the basic principle of 4Pi confocal fluorescence microscopy and shows the feasibility of such an instrument. The theoretical prediction is confirmed—that the response of the 4Pi confocal fluorescence microscope is within the envelope of the response of a confocal fluorescence microscope. The facts that the upper and lower elevations are 39% higher, the center peak 24% narrower, and the response of the confocal fluorescence microscope approximately 11% broader than calculated can be explained consistently by an apodization of the wave fronts that pass the objective lenses. This explanation is plausible because immersion oil objective lenses with an N.A. = 1.4 feature the largest technically possible aperture angle. Simple considerations on the focusing process (see Fig. 1) suggest that a decrease of the aperture causes the wave fronts to behave somewhat more as planar waves. This effect leads to a narrower central peak, a reduced distance between the first minima (for two planar waves a distance of $\lambda/2n = \sim 210$ nm is expected), and higher side elevations relative to the central peak. It is clear that in the limiting case of planar waves, the central peak and the side elevations reach equal heights. In addition, the shrinkage of the axial extent of the main maximum of the point spread-function with respect to its lateral extent is a high-numerical-aperture effect.[23] Furthermore, the calculations are based on a single wavelength of 725 nm, whereas the detected range is 665–820 nm. The latter and perhaps chromatic aberrations broaden the detection point-spread function and lead to increased side elevations and broader z discrimination. These phenomena have not been fully investigated, and more research in this field is needed.

When comparing the SNR of a confocal fluorescence microscope with that of a 4Pi confocal fluorescence microscope, we have to take into account the limited amount of fluorophore per unit volume and the maximum light intensity with which it is possible to illuminate without damaging the sample. Because of constructive interference of the two illumination wave fronts in a 4Pi confocal fluorescence microscope, the same maximal amplitude can be achieved when the objective lenses provide only one half of the illumination amplitude each. Thus only one fourth of the illumination intensity is needed for each objective. Since two wave fronts are used, the 4Pi confocal microscope requires only one half of the light to achieve the desired intensity in the focus. Thus the sample is exposed to only one half of the light, thereby yielding better protection against out-of-focus bleaching. Since the 4Pi microscope detects the light on both sides, the signal becomes twice as large. On the other hand, because of the enhanced resolution, the fluorescence light emanates from an object volume that is only one half of that in a confocal microscope. Therefore the 4Pi confocal fluorescence microscope is able to provide the same intensity and SNR as those of a confocal fluorescence microscope despite the fact that it probes a smaller volume. The 4Pi microscope currently available at the European Molecular Biology Laboratory loses 50% of the fluorescence emission, but this can be easily avoided with an improved arrangement.

The data presented in this paper show that a 4Pi microscope is feasible and has the properties that were expected. To exploit the full width at half-maximum of the central peak, one must reduce the heights of the upper and lower elevations or at least take them into account mathematically. An image would suffer from ghost images produced by these elevations. Changes in the phase of the two wave fronts force variations between constructive and destructive interference. Heterogeneity of the refractive index in the sample causes variations in the spot sizes and in the positions of the spots. However, the 4Pi microscope will always have a resolution that is better than that of a confocal fluorescence microscope.

A number of further approaches can be conceived that exploit the features of a 4Pi microscope: (a) The additional use of two-photon excitation introduces another intensity squaring.[24,25] The net effect is a reduction of the upper and lower elevations. (b) A possible reduction of the upper and lower elevations can also be achieved by applying suitable superresolving aperture filters. (c) The data can be deconvolved numerically since the information is well defined and the SNR is at least as good as that in a confocal fluorescence microscope. (d) Different combinations of (partly) destructive and (partly) constructive illumination point-spread functions are possible. (e) The phase difference of the two wave fronts can be modulated. Images are recorded as a function of phase and position along the optical axis, and this information is then used to estimate the actual phase and to deconvolve the images. This fifth approach seems to us the most promising, since it addresses all the problems mentioned above.

This paper is to our knowledge the first to prove the feasibility of resolution enhancement based on an increase of the numerical aperture in fluorescence microscopy. A fourfold increase of the axial resolution can be used to provide new insights into the structure and function of many organelles that are currently being investigated in modern cell biology. In conclusion, we believe that 4Pi confocal fluorescence microscopy has strong potential as a future instrument for three-dimensional light microscopy.

ACKNOWLEDGMENTS

S. Hell thanks the Deutsche Forschungsgemeinschaft (Bonn, Germany) for supporting his study on resolution enhancement in confocal microscopy with a postdoctoral fellowship. We thank Chr. Cremer for his constant interest and valuable discussions. K. Simons and S. Hunklinger supported this study during its earliest stages.

REFERENCES

1. T. Wilson, "Confocal microscopy," in *Confocal Microscopy*, T. Wilson, ed. (Academic, London, 1990).
2. M. Born and E. Wolf, *Principles of Optics*, 5th ed. (Pergamon, Oxford, 1975).
3. M. V. Klein and T. E. Furtak, *Optics*, 2nd ed. (Wiley, New York, 1986).
4. D. Gerlach, *Das Lichtmikroskop* (Georg Thieme Verlag, Stuttgart, 1976).
5. S. Hell, German patent application P40 40 441.2 (filed December 18, 1990; published 1992).

6. S. Hell, "The physical basis of confocal fluorescence microscopy," presented as part of the Scandinavian Course in Modern Image Analysis Technology, Jyvaskyla, Finland; Solubiologi **3,** 183–185 (1991).
7. S. Hell and E. H. K. Stelzer, "A 4Pi confocal microscope has an improved axial resolution," presented at the 4th International Conference on Confocal Microscopy, Amsterdam, The Netherlands, 1992.
8. C. J. R. Sheppard and Y. Gong, "Improvement in axial resolution by interference confocal microscopy," Optik **87,** 129–132 (1991).
9. K. Carlsson, P. E. Danielsson, R. Lenz, A. Liljeborg, L. Majlöf, and N. Åslund, "Three-dimensional microscopy using a confocal laser scanning microscope," Opt. Lett. **10,** 53–55 (1985).
10. R. W. Wijnaendts-van-Resandt, H. J. B. Marsman, J. Davoust, E. H. K. Stelzer, R. Stricker, "Optical Fluorescence microscopy in three dimensions," J. Microsc. **138,** 29–34 (1985).
11. G. J. Brakenhoff, H. T. M. van der Voort, E. A. Spronsen, and H. Nanninga, "Three-dimensional imaging by confocal scanning microscopy," Ann. N.Y. Acad. Sci. **483,** 405–415 (1986).
12. C. J. R. Sheppard and C. J. Cogswell, "Three-dimensional imaging in confocal microscopy," in *Confocal Microscopy,* T. Wilson, ed. (Academic, London, 1990).
13. T. Wilson and C. J. R. Sheppard, *Theory and Practice of Scanning Optical Microscopy* (Academic, London, 1984).
14. C. J. R. Sheppard and H. J. Matthews, "Imaging in high-aperture optical systems," J. Opt. Soc. Am. A **4,** 1354–1360 (1987).
15. B. Richards and E. Wolf, "Electromagnetic diffraction in optical systems, I. An integral representation of the image field." Proc. R. Soc. London Ser. A **253,** 349–357 (1959).
16. B. Richards and E. Wolf, "Electromagnetic diffraction in optical systems, II. Structure of the image field in aplanatic systems," Proc. R. Soc. London Ser. A **253,** 358–368 (1959).
17. A. Boivin, J. Dow, and E. Wolf, "Energy flow in the neighborhood of the focus of a coherent beam," J. Opt. Soc. Am. **57,** 1171–1175 (1967).
18. J. J. Stamnes, *Waves in Focal Regions* (Hilger, Bristol, England, 1986), p. 468.
19. H. T. M. van der Voort and G. J. Brakenhoff, "3-D image formation in high-aperture fluorescence confocal microscopy: a numerical analysis," J. Microsc. (Oxford) Pt. 1 **158,** 43–54, (1990).
20. S. Hell, E. Lehtonen and E. H. K. Stelzer, "Confocal fluorescence microscopy: wave optics considerations and applications to cell biology," in *New Dimensions of Visualization in Biomedical Microscopies,* A. Kriete, ed. (Verlag Chemie, Weinheim, Germany, 1992).
21. T. Wilson, "Optical sectioning in confocal fluorescent microscopes," J. Microsc. (Oxford) **154,** 143–156 (1989).
22. E. H. K. Stelzer and R. W. Wijnaendts-van-Resandt, "Optical cell slicing with the confocal fluorescence microscope: microtomoscopy," in *Confocal Microscopy,* T. Wilson, ed., (Academic, London, 1990).
23. S. Hell, "Abbildung transparenter Mikrostrukturen im konfokalen Mikroskop," Ph.D. dissertation (Universität Heidelberg, Heidelberg, Germany, 1990).
24. W. Denk, J. H. Strickler, and W. W. Webb, "Two-photon laser scanning fluorescence microscopy," Science **248,** 73–76 (1990).
25 S. Hell and E. H. K. Stelzer, "Fundamental improvement of resolution with a 4Pi-confocal microscope using two-photon excitation," Opt. Commun. (to be published).